water

MDPI

Article

Definition of the Operational Curves by Modification of the Affinity Laws to Improve the Simulation of PATs

Carlos Andrés Macías Ávila [1], Francisco-Javier Sánchez-Romero [2], P. Amparo López-Jiménez [1] and Modesto Pérez-Sánchez [1,*]

[1] Hydraulic and Environmental Engineering Department, Universitat Politècnica de València, 46022 Valencia, Spain; carmaav@posgrado.upv.es (C.A.M.Á.); palopez@upv.es (P.A.L.-J.)
[2] Rural and Agrifood Engineering Department, Universitat Politècnica de València, 46022 Valencia, Spain; fcosanro@agf.upv.es
* Correspondence: mopesan1@upv.es

Abstract: New technologies for water pressurized systems try to implement the introduction of strategies for the improvement of the sustainable indicators. One of these technologies is the implementation of pumps working as turbines. The use of these recovery machines was proposed some years ago, and the interest in this technology has increased over the last years. The simulation of these machines is necessary when analyzing pressurized water systems, or when optimization procedures are proposed for their management, great care must be taken. In these cases, the knowledge of the operation curves is crucial to reach accurate results. This study proposes different regression expressions to define three operational curves when the machines operate under variable rotational speed. These curves are the best efficiency head, the best power-head and the best power flow. The here proposed methods were compared with other five published methods. The comparison shows the proposed method was the best when it is compared with the rest of the published procedures, reducing the error values between 8 and 20%.

Keywords: variable rotational speed; affinity laws; PATs; water networks; energy recovery

Citation: Macías Ávila, C.A.; Sánchez-Romero, F.-J.; López-Jiménez, P.A.; Pérez-Sánchez, M. Definition of the Operational Curves by Modification of the Affinity Laws to Improve the Simulation of PATs. *Water* **2021**, *13*, 1880. https://doi.org/10.3390/w13141880

Academic Editor: Costanza Aricò

Received: 17 June 2021
Accepted: 5 July 2021
Published: 6 July 2021

1. Introduction

The use of micro-hydropower systems is key to improve the energy efficiency in water pressurized systems. The accuracy of the energy analyses is also very important in the complete analysis of these energy improvements [1]. Pump working as turbines (PATs) are hydraulic machines, which are commonly recommended to be used as recovery machines in water pressurized systems [2]. These favorable aspects were defined by different published researches in which the feasibility, simple operation, availability in the market and great range of applications are some of the most important characteristics of these systems, when they are compared with classical machines such as Francis or Pelton turbine. However, the use of these recovery machines has the main disadvantage joined to low efficiency compared to classical machines [3]. The knowledge of their characteristic curves (i.e., head, efficiency and power) is difficult to know in advance if water managers look in the manufacturer catalogue.

The lack of this information has been a challenge, in which researchers tried to fill this shortage by proposing empirical expressions [4]. These functions are based on the development of the experimental tests. These helped to understand better the operating of these machines when these recovery systems operate as turbine [5]. The need to establish these equations are focused on two main aspects: (i) the knowledge of the best operation point of the machine (*BEP*) when it operates as turbine and the water manager only knows the characteristic curves in pump mode; and (ii) the need to regulate the rotational speed of the machine to maximize the recovered energy of the system when variable operation strategy is applied.

The first challenge was studied by different researchers. Ref. [6] established a common empirical equation to estimate the best efficiency point of the machine when it operates as a turbine from a pump. These expressions and the empirical equations proposed by [7] are the most used last years. However, other published researches focused on their effort to improve these expressions. Ref. [8] proposed computational fluid dynamics analysis to characterize and improve the accuracy of these methods, which tried to predict the operational point. Different methods were reviewed by [9], who proposed empirical expressions using the greater database, particularly 181 different PATs. The proposed expressions estimated the *BEP* operation as a turbine with errors lower than the rest of the methods reviewed by [3]. In this line, Ref. [10] defined regression expression to estimate the curve of head and efficiency when the rotational speed changes by modification of the affinity laws, improving the results obtained in others researches [11].

The use of these empirical equations focuses on improving the simulation of PAT systems operating under variable rotational speed. Ref. [2] showed the need to know these curves in the energy estimation strategies in the water systems. The analysis of the hydropower potential contributes to incorporate sustainable measurements in which the water-energy nexus acquires relevance in the water management of the systems [12]. When micro-hydropower systems are analyzed, the effectiveness increases when the variable operation strategy (*VOS*) is applied [13]. Therefore, the improvement in the estimation of the operational curves makes sense to search for the best strategy to maximize the recovered energy by the recovery system [14].

The knowledge of expressions, which allow water managers to use with software and optimization procedure will improve the decision making in the water systems [15]. The future strategies should be focused on improving sustainability as well as the alignment of the operation indicators with the sustainable development goals [16]. The research is focused on the development of regression expressions. These equations define the generated power as a function of the flow under variable rotational speed. These curves are: (i) the best efficiency head, proposed by [17] and (ii) the best power curve proposed in this research, which is key in the maximization of energy. Besides, the research compiles the great database used by researchers to analyze the PATs systems operating under variable rotational speed. This research considers 15 different machines, which were tested on 87 different rotational speeds. The proposed regression equations, which are based on non-dimensional parameters is validated by the error analysis compared to other published methods, obtaining better approaches.

2. Material and Methods

2.1. Hydraulic Mathematical Development

The modification of the affinity laws is recommendable when the characteristic curves must be estimated by water managers, *n* accordance with the aforementioned references. The characteristics curves are head curve (*HC*), efficiency curve (*EC*) and power curve (*PC*). These curves are defined by the following expression:

$$H_0 = A + BQ_0 + CQ_0^2 \quad (1)$$

$$\eta_0 = E_4Q_0^4 + E_3Q_0^3 + E_2Q_0^2 + E_1Q_0 + E_0 \quad (2)$$

$$P_0 = P_4Q_0^4 + P_3Q_0^3 + P_2Q_0^2 + P_1Q_0 + \mathrm{P}_5 \quad (3)$$

where H_0 is the recovered head in nominal rotational speed in m w.c. (water column); Q_0 is the flow rate in m^3/s; η_0 is the efficiency of the machine; P_0 is the generated power in kW. The rest of the coefficients (A, B, C, E_4,E_3,E_2, E_1, E_0, P_4, P_3,P_2, P_1 and P_5) are the coefficients, which define the *HC*, *EC* and *PC* of the pump working as the turbine.

The variation of the rotational speed is defined by affinity laws when classical concepts are considered. The definition of the affinity laws is based on the analysis of the congruence parabola (H_{CP}), which was defined and applied by [18]. This parabola is defined by the following expression:

$$H_{CP} = \frac{H_0}{Q_0^2} Q^2 = k_{H,AL} Q^2 \quad (4)$$

Considering an operation point (Q_0, H_0), when the congruence parabola concept is applied, the affinity laws are defined by the following expressions [18]:

$$\frac{Q_1}{Q_0} = \frac{n_1}{n_0} = \alpha \quad (5)$$

$$\frac{H_1}{H_0} = \left(\frac{n_1}{n_0}\right)^2 = \alpha^2 \quad (6)$$

$$\frac{\eta_1}{\eta_0} = 1 \quad (7)$$

$$\frac{P_1}{P_0} = \left(\frac{n_1}{n_0}\right)^3 = \alpha^3 \quad (8)$$

where n_1 is the new rotational speed in rpm, n_0 is the nominal rotational speed in rpm; Q_1 is the circulating flow when the rotational speed is n_1; H_1 is the recovered head when the machine operates for a flow equal to Q_1 in m w.c.; η_1 is the new efficiency of the machine when it operates in Q_1.

Different published researches established the need to modify these affinity laws to better address the estimation of the characteristics curves of the machine. These affinity laws can be defined using dimensionless numbers of the machines (q, h, e and p) [19], which enable the establishment of the operation function for determining any rotational speed.

$$q = \frac{Q}{Q_0} \quad (9)$$

$$h = \frac{H}{H_0} \quad (10)$$

$$e = \frac{\eta}{\eta_0} \quad (11)$$

$$p = \frac{P}{P_0} = qhe \quad (12)$$

where q, h, e *and* p are operation functions for different rotational speed (α), Q is any flow value of PAT in m^3/s. This value is inside of the *VOS*; H is the recovered head for this flow in m w.c. when the machine operates at the ratio of rotational speed equal to α; η is the efficiency for values of Q, H and α; P is the shaft power in this operation point in kW; Q_0, H_0, P_0 and η_0 are referred to any point of the characteristic curve of the machine when it is operating at nominal rotational speed (i.e., $\alpha = 1$).

The curves for any rotational speed inside of the *VOS* were defined by [10], who established the following expressions:

$$H = h\left(A + B\frac{Q}{q} + C\left(\frac{Q}{q}\right)^2\right) \quad (13)$$

$$\eta = e\left(E_4\left(\frac{Q}{q}\right)^4 + E_3\left(\frac{Q}{q}\right)^3 + E_2\left(\frac{Q}{q}\right)^2 + E_1\left(\frac{Q}{q}\right) + E_0\right) \quad (14)$$

$$P = p\left(P_4\left(\frac{Q}{q}\right)^4 + P_3\left(\frac{Q}{q}\right)^3 + P_2\left(\frac{Q}{q}\right)^2 + P_1\left(\frac{Q}{q}\right) + P_5\right) \quad (15)$$

This relationship between q and Q is linear and it is determined by the slope m. The m value will adopt a constant value according to the curve analyzed (best efficiency head, *BEH*; best power head, *BPH* or best power flow, *BPF*) [19,20]. Any value of Q_0 has an associated line, which has a slope equal to m (Figure 1a).

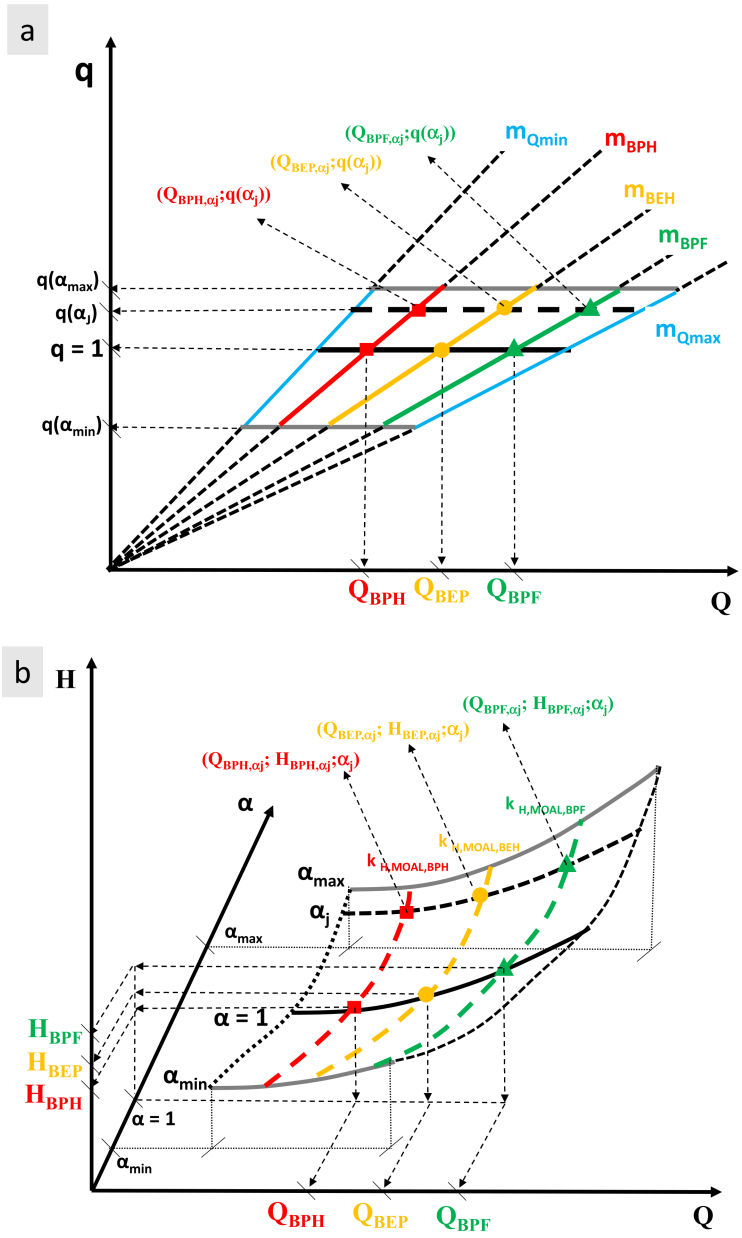

Figure 1. (**a**) m coefficient; (**b**) VOS zone.

The m value remains constant either in affinity laws or modified affinity laws, changing the q expression. When the *VOS* is defined by affinity laws, q is equal to α. If the modified affinity laws (*MOAL*) are used, q is a function both α and $\frac{Q}{Q_{BEP}}$ [10]. The m value is defined by the following expression:

$$m = \frac{1}{Q_0} \tag{16}$$

$$q = mQ_0 \tag{17}$$

The m parameter enables to simplify the development of expressions, which are used to develop the expression when a machine operates under variable rotational speed.

The variation of the rotational speed inside of the *VOS* is defined by the previously cited congruence parabola (*CP*). This *CP* enables to define the change the rotational speed. Besides, when these *CP*s are used, they help to define the analytical curves of the characteristic curves (head, efficiency and power) both the application of the affinity laws and modified affinity laws (Figure 1b). These new curves were called the modified affinity laws (*MOAL*) [20–22]. When coefficients of the congruence parabola (k_i) are operated comparing between affinity laws (*AL*) and modified affinity laws, the following expressions are obtained. The modification of these expressions is defined in Table 1.

Table 1. Definition of the curves as a function of k_i parameter.

Curve	Curve Type	AL	MOAL
Head	$H = k_H Q^2$	$k_{H,AL} = \frac{H_0}{Q_0^2} = (Am^2 + Bm + C)$	$k_{H,MOAL} = \frac{h}{q^2} k_{H,AL}$
Efficiency	$\eta = e\eta_0$	$\eta_{AL} = \eta_0$	$\eta_{MOAL} = e \cdot \eta_{AL}$
		Using head and efficiency curves $k_{P,AL} = 9.81 \cdot k_{H,AL} \cdot \eta_{AL}$	$k_{P,MOAL} = \frac{he}{q^2} k_{P,AL}$
Power	$P = k_P Q^3$	Using power expression $k_{P,AL} = \frac{P_0}{Q_0^3}$ $k_{P,AL} = \left(\frac{P_4}{m} + P_3 + P_2 m + P_1 m^2 + P_5 m^3\right)$	$k_{P,MOAL} = \frac{p}{q^3} k_{P,AL} = \frac{he}{q^2} k_{P,AL}$

Each congruence parabola has one m parameter, which is associated to an α value. The m parameter enables the estimation of the curves H-Q, η-Q and P-Q, directly. This m is the unknown value, and it should be solved for the different operational curves inside of the *VOS* zone. Once, m or Q_0 are known, the estimation of the characteristic curves is possible and therefore, the definition of the following curves is feasible.

Best efficiency head (BEH), defined by [18], this curve is the line, which establishes the α value in which the efficiency is maximum for a defined flow. The analysis of this equation is defined in the following:

$$\frac{d\eta}{d\alpha} = 0 \tag{18}$$

Considering Equations (2), (5) and (9):

$$\frac{d\eta}{d\alpha} = \frac{d(E_4\left(\frac{Q}{\alpha}\right)^4 + E_3\left(\frac{Q}{\alpha}\right)^3 + E_2\left(\frac{Q}{\alpha}\right)^2 + E_1\left(\frac{Q}{\alpha}\right) + E_0)}{d\alpha} = 0 \tag{19}$$

As the relationship between α and Q is $\alpha = m\ Q$, considering Equations (16) and (17), the expression enables to calculate the m parameter is:

$$E_1 m^3 + 2E_2 m^2 + 3E_3 m + 4E_4 = 0 \tag{20}$$

Best power head (BPH), this curve is the line, which establishes the α value in which the power is maximum for a defined flow [20,21]. The analysis of this equation is defined in the following

$$\frac{dP}{d\alpha} = 0 \tag{21}$$

Considering Equations (1), (2), (5) and (9):

$$\frac{dP}{d\alpha} = \frac{d(9.81Q\alpha^2(A + B\frac{Q}{\alpha} + C\left(\frac{Q}{\alpha}\right)^2)(E_4\left(\frac{Q}{\alpha}\right)^4 + E_3\left(\frac{Q}{\alpha}\right)^3 + E_2\left(\frac{Q}{\alpha}\right)^2 + E_1\left(\frac{Q}{\alpha}\right) + E_0))}{d\alpha} = 0 \tag{22}$$

As the relationship between α and Q is $\alpha = m\ Q$, considering Equations (16) and (17), the expression enables to calculate the m parameter is:

$$(2E_0A)m^6 + (E_0B + E_1A)m^5 + (-E_1C - E_2B - E_3A)m^3 + (-2E_2C - 2E_3B - 2E_4A)m^2 + (-3E_3C - 3E_4B)m + (-4E_4C) = 0 \tag{23}$$

Best power flow (BPF), this curve is the line, which establishes the Q value in which the power is maximum for a defined α. The analysis of this equation is defined in the following

$$\frac{dP}{dQ} = 0 \tag{24}$$

Considering Equations (1), (2), (5) and (9):

$$\frac{dP}{dQ} = \frac{d(9.81Q\alpha^2(A + B\frac{Q}{\alpha} + C\left(\frac{Q}{\alpha}\right)^2)(E_4\left(\frac{Q}{\alpha}\right)^4 + E_3\left(\frac{Q}{\alpha}\right)^3 + E_2\left(\frac{Q}{\alpha}\right)^2 + E_1\left(\frac{Q}{\alpha}\right) + E_0))}{dQ} = 0 \tag{25}$$

As the relationship between α and Q is $\alpha = m\ Q$, considering Equations (16) and (17), the expression enables to calculate the m parameter is:

$$(E_0A)m^6 + 2(E_0B + E_1A)m^5 + 3(E_0C + E_1B + E_2A)m^4 + 4(E_1C + E_2B + E_3A)m^3 + 5(E_2C + E_3B + E_4A)m + 6(E_3C + E_4B)m + 7E_4C = 0 \tag{26}$$

Once, the three curves (*BEH*, *BPH* and *BPF*) are known, the knowledge of the m parameter is demonstrated it can be solved by a polynomial equation, which has the next typology:

$$\gamma_6 m^6 + \gamma_5 m^5 + \gamma_4 m^4 + \gamma_3 m^3 + \gamma_2 m^2 + \gamma_1 m + \gamma_0 = 0 \tag{27}$$

Table 2 summarizes the value of the different coefficients for *BEH*, *BPH* and *BPF* as a function of the characteristic curve when they operate in nominal conditions. The introduction of the 'm' parameter simplifies the analysis of the mathematical expressions that allow to study of the behaviour of the machines along the *VOS* zone, facilitating the analysis in situations different from the nominal regime.

Table 2. Coefficients for the knowledge of the m parameters.

Curve	*BEH*	*BPH*	*BPF*
Restriction	$\frac{d\eta}{d\alpha} = 0$	$\frac{dP}{d\alpha} = 0$	$\frac{dP}{dQ} = 0$
γ_6	0	$2E_0A$	E_0A
γ_5	0	$E_0B + E_1A$	$2(E_0B + E_1A)$
γ_4	0	0	$3(E_0C + E_1B + E_2A)$
γ_3	E_1	$-E_1C - E_2B - E_3A$	$4(E_1C + E_2B + E_3A)$
γ_2	$2E_2$	$-2E_2C - 2E_3B - 2E_4A$	$5(E_2C + E_3B + E_4A)$
γ_1	$3E_3$	$-3E_3C - 3E_4B$	$6(E_3C + E_4B)$
γ_0	$4E_4$	$-4E_4C$	$7E_4C$
Solution	m_{BEH}	m_{BPH}	m_{BPF}

2.2. Methodology

The proposed methodology is based on ten different steps (Figure 2). This figure contains two different phases. The first phase analyses the experimental database from Steps A to D. The second phase considers the analytical procedure to define the best equation to establish the operation curves of the machine from Steps E to J.

Step A. Using the different experimental database, the characteristic curves are obtained for each machine as well as considering different rotational speeds.

Step B. When the curves are known, the procedure determines the flow for the different curves when the machine operates on nominal rotational speed. The flow values are: (i) best efficiency head (Q_{BEH}), (ii) best power head (Q_{BPH}), and (iii) best power flow (Q_{BPF}).

Step C. Defined the three flow values in step B, the procedure defines these flow values for the different values of the rotational speed (α_j), which were tested experimentally. Therefore, Q_{BEH,α_j}, Q_{BPH,α_j} and Q_{BPF,α_j} are determined.

Step D. The non-dimensional parameters, $\left(h/q^2\right)_{Exp}$ and $\left(he/q^2\right)_{Exp}$, are defined using the experimental database for different values of the rotational speed.

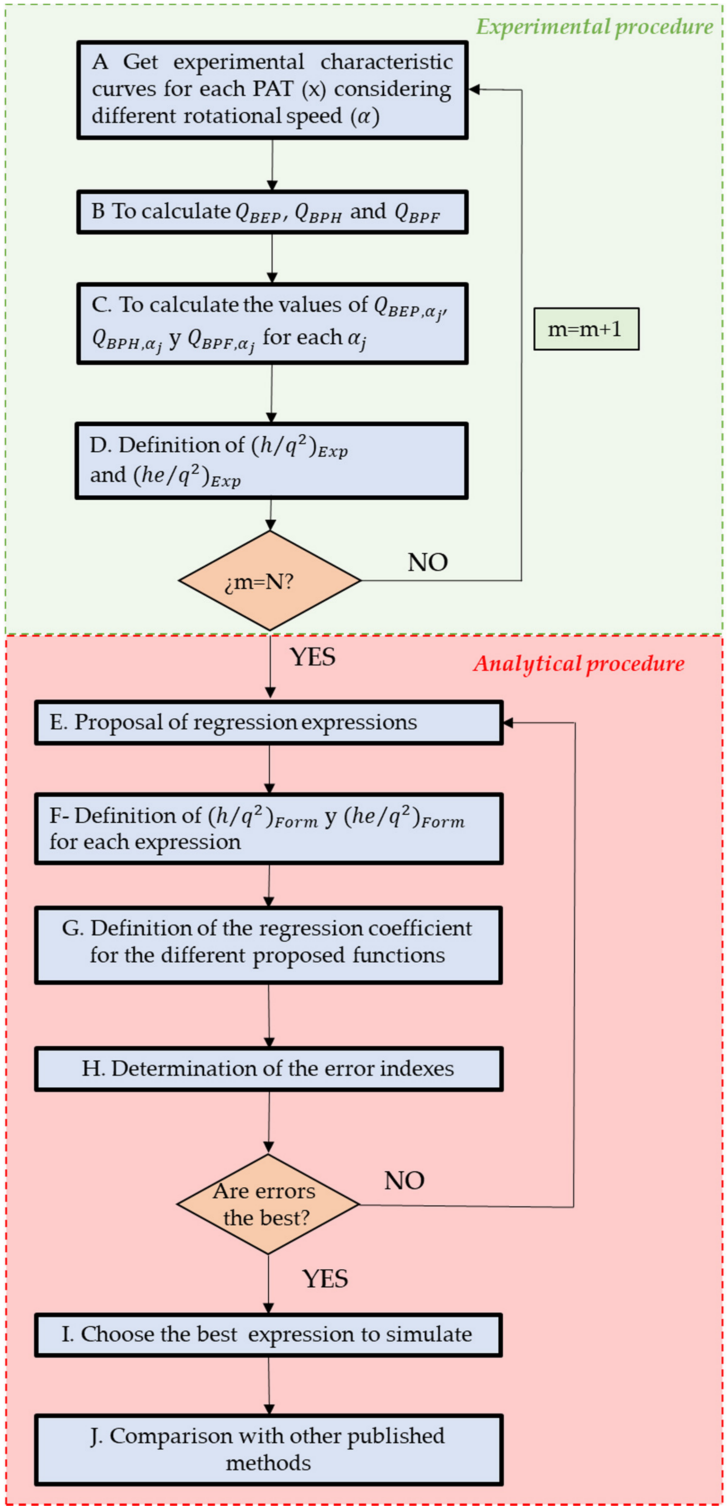

Figure 2. The methodology proposed to reach the expressions.

Step E. It is the first step of the second phase, where the best regression expression will be defined. In this step, different functions are proposed and analysed using the database. Table 3 shows the regression expression, which is used in the procedure.

Table 3. Proposed functions to be analysed.

Function Model (FM)	Polynomial function (From F_1 to F_6): $NP=\beta_1\left(\alpha\frac{Q}{Q_{BEP}}\right)+\beta_2\left(\frac{Q}{Q_{BEP}}\right)^2+\beta_3\left(\frac{Q}{Q_{BEP}}\right)+\beta_4\alpha^2+\beta_5\alpha+\beta_6$ Potential function (From F_7 to F_{10}): $NP=\left(\frac{Q}{Q_{BEP}}\right)^{\beta_3}\alpha^{\beta_5}\cdot exp^{\beta_6}$
F_1	$NP=\beta_4\alpha^2+\beta_5\alpha$
F_2	$NP=\beta_4\alpha^2+\beta_5\alpha+\beta_6$
F_3	$NP=\beta_2\left(\frac{Q}{Q_{BEP}}\right)^2+\beta_4\alpha^2+\beta_5\alpha$
F_4	$NP=\beta_2\left(\frac{Q}{Q_{BEP}}\right)^2+\beta_4\alpha^2+\beta_5\alpha+\beta_6$
F_5	$NP=\beta_1\left(\alpha\frac{Q}{Q_{BEP}}\right)+\beta_2\left(\frac{Q}{Q_{BEP}}\right)^2+\beta_3\left(\frac{Q}{Q_{BEP}}\right)+\beta_4\alpha^2+\beta_5\alpha$
F_6	$NP=\beta_1\left(\alpha\frac{Q}{Q_{BEP}}\right)+\beta_2\left(\frac{Q}{Q_{BEP}}\right)^2+\beta_3\left(\frac{Q}{Q_{BEP}}\right)+\beta_4\alpha^2+\beta_5\alpha+\beta_6$
F_7	$NP=\alpha^{\beta_5}$
F_8	$NP=\alpha^{\beta_5}\cdot exp^{\beta_6}$
F_9	$NP=\left(\frac{Q}{Q_{BEP}}\right)^{\beta_3}\alpha^{\beta_5}$
F_{10}	$NP=\left(\frac{Q}{Q_{BEP}}\right)^{\beta_3}\alpha^{\beta_5}\cdot exp^{\beta_6}$

NP is the non-dimensional parameter. It can be $\frac{h}{q^2}$ or $\frac{he}{q^2}$

Step F. Once the proposed regression expression is defined in the previous step, the values of $(h/q^2)_{Form}$ and $(he/q^2)_{Form}$ are estimated for each F_i, defining the error indexes, which enable to choose of the best regression expression to define the proposed functions (*BEH*, *BPH* and *BPF*).

Step G. Definition of the regression expression for $\frac{h}{q^2}$ and $\frac{he}{q^2}$.

Step H. The error indexes were estimated for each function when the dimensionless parameters ($\frac{h}{q^2}$ and $\frac{he}{q^2}$) were applied to *BEH*, *BPH* and *BPF*. The error indexes are defined in Table 4.

Table 4. Error indexes used in the analysis.

Error Index	Equation	Variable	Accuracy
Root Mean Square Error (*RMSE*)	$RMSE=\sqrt{\frac{\sum_{i=1}^{s}[O_i-P_i]^2}{s}}$	O_i are the estimated values; P_i the experimental values and s the number of observations	Perfect fit when *RMSE* is zero
Mean Absolute Deviation (*MAD*)	$MAD=\sum_{1}^{s}\frac{1}{s}\lvert O_i-P_i\rvert$	O_i are the estimated values; P_i the experimental values and s the number of observations	Perfect fit when *MAD* is zero
Mean Relative Deviation (*MRD*)	$MRD=\sum_{1}^{s}\frac{\lvert O_i-P_i\rvert/P_i}{s}$	O_i are the estimated values; P_i the experimental values and s the number of observations	
BIAS	$BIAS=\frac{\sum_{i=1}^{s}[O_i-P_i]}{s}$	O_i are the estimated values; P_i the experimental values and s the number of observations	Perfect fit is zero

Step I. The function, which minimizes the errors is defined to establish the *BEH*, *BPH* and *BPF*.

Step J. The chosen function is compared with other published methods, comparing the error indexes, which were defined in Step H to show the accuracy between this study, other published methods and experimental tests when *BEH*, *BPH* and *BPQ* are defined both analytical and experimental.

2.3. Materials

The analytical development described here was applied to different machines, which were tested in different published experimental tests. In this case, the used machines were fifteen PATs, which have a specific speed between 5.67 and 50.71 rpm (m, kW). The nominal rotational speed was between 800 and 3000 rpm. The non-dimensional curves of the machines are shown in Figure 3. The number of experimental curves (RS) was 87. These curves were tested for different rotational speed. The use of the experimental data enabled to interpolation of more than 10,000 parabolas. All curves were used to define the regression expressions except ID11, which was used to compare the empirical equations with the experimental data.

Id	n_0 (rpm)	D (mm)	Q_{BEP} (l/s)	H_{BEP} (m	η_{BEP}	RS	Id	n_0 (rpm)	D (mm)	Q_{BEP} (l/s)	H_{BEP} (m w.c.)	η_{BEP}	RS
1	1020	139	3.461	4.144	0.615	4	9	1100	193	9.762	51.267	0.703	6
2	1200	200	24.46	12.44	0.596	7	10	3000	127	17.99	30.288	0.695	6
3	1100	225	22.3	11.94	0.714	7	11	3000	158	17.98	51.355	0.727	6
4	1100	250	23.73	11.91	0.766	7	12	2700	127	36.91	22.207	0.705	7
5	1200	210	16.76	18.13	0.718	6	13	1000	419	95.59	34.428	0.795	4
6	800	265	27.32	8.305	0.800	5	14	1250	175	8.99	17.525	0.622	6
7	1200	255	28.39	15.86	0.715	6	15	2900	189	50.05	52.849	0.646	7
8	1200	139	4.906	11.28	0.543	3						Total	87

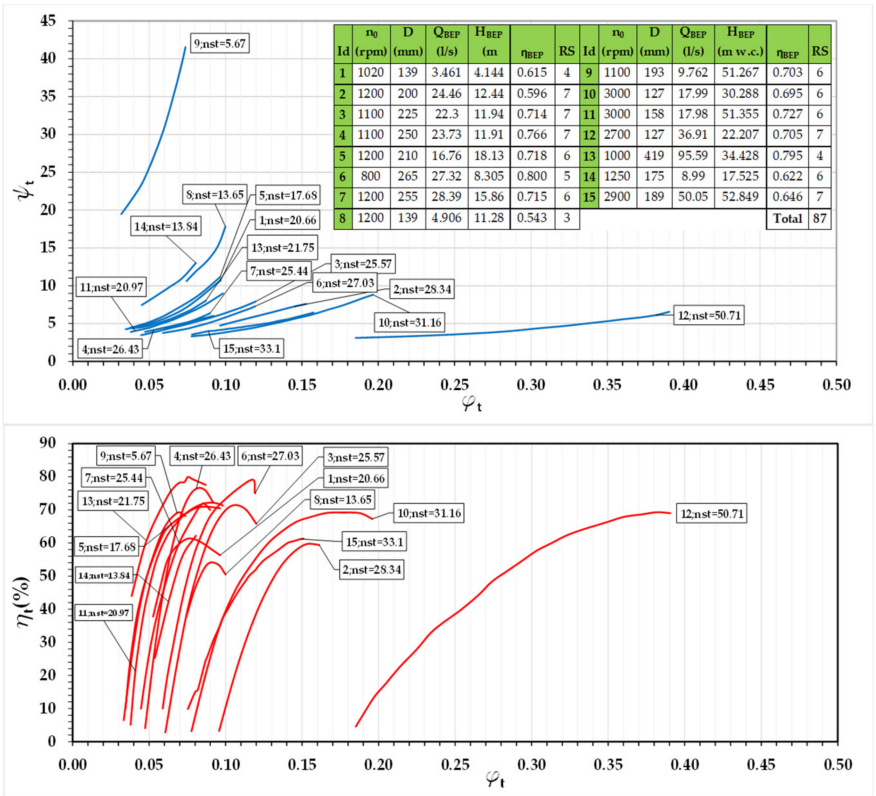

Figure 3. Experimental database. Experimental database. ID1 [23]; ID2-ID4 [24]; ID5-ID7 [21]; ID8 [25]; ID9 [26]; ID10-ID12 [27]; ID13 [28]; ID14 [2]; ID15 [3].

3. Results

3.1. Definition of the Regression Expression to Define F_i

The regression expressions propose for $\frac{h}{q^2}$ and $\frac{he}{q^2}$ are shown in Table 5. It shows the different values of the β_i for each function F_i. These ten functions are used to estimate the *BEH*, *BPH* and *BPF* curves using the $\frac{h}{q^2}$ and $\frac{he}{q^2}$ the dimensionless coefficient for each machine. The estimation considered all experimental rotational speed of the PATs, considering their characteristic curves.

Table 5. Proposed expression for the dimensionless numbers.

Function Model (FM)	Expressions
F_1	$\frac{h}{q^2} = -0.512\alpha^2 + 1.63\alpha \ (R^2 = 0.978)$
	$\frac{he}{q^2} = -0.826\alpha^2 + 1.843\alpha \ (R^2 = 0.979)$
F_2	$\frac{h}{q^2} = 1.048\alpha^2 - 1.487\alpha + 1.469 \ (R^2 = 0.738)$
	$\frac{he}{q^2} = -0.1706\alpha^2 + 0.5336\alpha + 0.617 \ (R^2 = 0.151)$
F_3	$\frac{h}{q^2} = -0.235\left(\frac{Q}{Q_{BEP}}\right)^2 - 0.5196\alpha^2 + 1.789\alpha \ (R^2 = 0.981)$
	$\frac{he}{q^2} = -0.024\left(\frac{Q}{Q_{BEP}}\right)^2 - 0.826\alpha^2 + 1.858\alpha \ (R^2 = 0.979)$
F_4	$\frac{h}{q^2} = -0.1139\left(\frac{Q}{Q_{BEP}}\right)^2 + 0.965\alpha^2 - 1.254\alpha + 1.395 \ (R^2 = 0.764)$
	$\frac{he}{q^2} = 0.032\left(\frac{Q}{Q_{BEP}}\right)^2 - 0.148\alpha^2 + 0.469\alpha + 0.637 \ (R^2 = 0.154)$
F_5	$\frac{h}{q^2} = -1.508\left(\alpha\frac{Q}{Q_{BEP}}\right) - 0.471\left(\frac{Q}{Q_{BEP}}\right)^2 + 1.93\left(\frac{Q}{Q_{BEP}}\right) + 0.714\alpha^2 + 0.342\alpha \ (R^2 = 0.986)$
	$\frac{he}{q^2} = 0.532\left(\alpha\frac{Q}{Q_{BEP}}\right) - 0.828\left(\frac{Q}{Q_{BEP}}\right)^2 + 0.757\left(\frac{Q}{Q_{BEP}}\right) - 0.757\alpha^2 + 1.287\alpha \ (R^2 = 0.98)$
F_6	$\frac{h}{q^2} = -0.69\left(\alpha\frac{Q}{Q_{BEP}}\right) + 0.122\left(\frac{Q}{Q_{BEP}}\right)^2 + 0.313\left(\frac{Q}{Q_{BEP}}\right) + 1.222\alpha^2 - 1.267\alpha + 1.294 \ (R^2 = 0.778)$
	$\frac{he}{q^2} = 0.993\left(\alpha\frac{Q}{Q_{BEP}}\right) - 0.494\left(\frac{Q}{Q_{BEP}}\right)^2 - 0.156\left(\frac{Q}{Q_{BEP}}\right) - 0.471\alpha^2 + 0.38\alpha + 0.73 \ (R^2 = 0.191)$
F_7	$\frac{h}{q^2} = \alpha^{0.214} \ (R^2 = 0.207)$
	$\frac{he}{q^2} = \alpha^{0.245} \ (R^2 = 0.175)$
F_8	$\frac{h}{q^2} = \alpha^{0.305} \cdot exp^{0.077} \ (R^2 = 0.402)$
	$\frac{he}{q^2} = \alpha^{0.202} \cdot exp^{-0.036} \ (R^2 = 0.116)$
F_9	$\frac{h}{q^2} = \left(\frac{Q}{Q_{BEP}}\right)^{-0.23} \alpha^{0.451} \ (R^2 = 0.506)$
	$\frac{he}{q^2} = \left(\frac{Q}{Q_{BEP}}\right)^{0.11} \alpha^{0.132} \ (R^2 = 0.22)$
F_{10}	$\frac{h}{q^2} = \left(\frac{Q}{Q_{BEP}}\right)^{-0.166} \alpha^{0.422} \cdot exp^{0.032} \ (R^2 = 0.478)$
	$\frac{he}{q^2} = \left(\frac{Q}{Q_{BEP}}\right)^{0.083} \alpha^{0.143} \cdot exp^{-0.013} \ (R^2 = 0.129)$

When these curves are defined, the error indexes were calculated comparing them with each experimental value and calculating the mean value (Tables 6 and 7). Table 6 shows the average error indexes when the non-dimensional parameter, $\frac{h}{q^2}$, was calculated for the different 10 proposed functions. When the *BEH* curve is analysed, the function which showed the minimum average error was F_2. *RMSE*, *MAD* and *MRD* were 0.1035, 0.0735 and 0.0628, respectively. However, the second function was F_6, which the error difference was 2.4% and 4.7% for *RMSE* and *MAD* respectively, while the *MRD* was better for F_2, reducing a −0.94% compared to F_2.

Table 6. Average error indexes for $\frac{h}{q^2}$ applied.

BEH					***BPH***					***BPF***				
FM	RMSE	MAD	MRD	BIAS	FM	RMSE	MAD	MRD	BIAS	FM	RMSE	MAD	MRD	BIAS
F_1	0.1515 (9)	0.1144 (9)	0.1023 (10)	−0.04 (3)	F_1	0.1863 (8)	0.1354 (10)	0.1136 (10)	−0.0356 (5)	F_1	0.1393 (7)	0.1059 (7)	0.0964 (8)	−0.0238 (3)
F_2	0.1035 (1)	0.0735 (1)	0.0628 (2)	−0.0172 (1)	F_2	0.1537 (3)	0.1107 (3)	0.0917 (7)	−0.0128 (1)	F_2	0.0959 (1)	0.0708 (1)	0.0629 (1)	−0.001 (1)
F_3	0.1636 (10)	0.1154 (10)	0.0999 (9)	−0.0966 (10)	F_3	0.1882 (9)	0.1321 (9)	0.1055 (9)	−0.0585 (8)	F_3	0.2115 (9)	0.1709 (9)	0.1515 (9)	−0.1634 (9)
F_4	0.1134 (3)	0.0819 (3)	0.0695 (3)	−0.0441 (5)	F_4	0.1531 (2)	0.1106 (2)	0.0898 (6)	−0.0249 (2)	F_4	0.119 (4)	0.0957 (6)	0.0838 (6)	−0.0635 (5)

Table 6. *Cont.*

	BEH					***BPH***					***BPF***			
F_5	0.1398 (7)	0.0974 (7)	0.0778 (7)	−0.0755 (7)	F_5	0.1924 (10)	0.1275 (8)	0.0954 (8)	−0.0754 (9)	F_5	0.3517 (10)	0.257 (10)	0.2114 (10)	−0.2302 (10)
F_6	0.1077 (2)	0.0755 (2)	0.0622 (1)	−0.0408 (4)	F_6	0.1479 (1)	0.1043 (1)	0.0819 (2)	−0.0313 (4)	F_6	0.1056 (2)	0.079 (2)	0.0664 (2)	−0.0432 (4)
F_7	0.1341 (6)	0.0927 (6)	0.074 (6)	−0.0865 (8)	F_7	0.1641 (5)	0.1116 (4)	0.0813 (1)	−0.082 (10)	F_7	0.1213 (5)	0.0844 (4)	0.0676 (3)	−0.0703 (6)
F_8	0.1194 (4)	0.0865 (4)	0.0727 (5)	−0.0308 (2)	F_8	0.1596 (4)	0.1127 (5)	0.0887 (4)	−0.0263 (3)	F_8	0.1146 (3)	0.0828 (3)	0.0712 (4)	−0.0146 (2)
F_9	0.1418 (8)	0.0998 (8)	0.0819 (8)	−0.0929 (9)	F_9	0.1719 (7)	0.1171 (7)	0.0895 (5)	−0.0543 (7)	F_9	0.149 (8)	0.1128 (8)	0.0951 (7)	−0.1052 (8)
F_{10}	0.1289 (5)	0.0885 (5)	0.0724 (4)	−0.0673 (6)	F_{10}	0.1654 (6)	0.1138 (6)	0.088 (3)	−0.0386 (6)	F_{10}	0.1265 (6)	0.0879 (5)	0.0725 (5)	−0.0721 (7)

(x) indicated the position when the error is considered and compared between functions.

Table 7. Average error indexes for $\frac{he}{q^2}$.

	BEH					***BPH***					***BPF***			
FM	RMSE	MAD	MRD	BIAS	FM	RMSE	MAD	MRD	BIAS	FM	RMSE	MAD	MRD	BIAS
F_1	0.1 (9)	0.0741 (9)	0.0766 (9)	−0.0269 (8)	F_1	0.0754 (8)	0.0529 (8)	0.0549 (8)	−0.0241 (8)	F_1	0.1502 (8)	0.1162 (7)	0.1206 (6)	−0.0139 (5)
F_2	0.073 (6)	0.056 (6)	0.0582 (6)	−0.0173 (6)	F_2	0.0523 (3)	0.0386 (3)	0.0398 (2)	−0.0145 (5)	F_2	0.1438 (6)	0.1111 (4)	0.1183 (3)	−0.0043 (1)
F_3	0.1017 (10)	0.075 (10)	0.0771 (10)	−0.0326 (10)	F_3	0.0763 (9)	0.0536 (9)	0.0553 (9)	−0.0264 (9)	F_3	0.1529 (9)	0.1171 (9)	0.1193 (5)	−0.0279 (7)
F_4	0.0702 (5)	0.054 (5)	0.0568 (5)	−0.0099 (4)	F_4	0.0534 (4)	0.0407 (4)	0.0424 (4)	−0.0111 (4)	F_4	0.1415 (2)	0.1111 (3)	0.1213 (7)	0.013 (4)
F_5	0.0972 (8)	0.0723 (8)	0.0737 (8)	−0.0307 (9)	F_5	0.0849 (10)	0.0631 (10)	0.0649 (10)	−0.0301 (10)	F_5	0.2814 (10)	0.2218 (10)	0.2061 (10)	−0.1608 (10)
F_6	0.0677 (3)	0.0513 (1)	0.0539 (1)	−0.0138 (5)	F_6	0.0467 (1)	0.0356 (1)	0.0371 (1)	−0.0054 (2)	F_6	0.1433 (4)	0.1129 (5)	0.1164 (2)	−0.0407 (9)
F_7	0.0669 (2)	0.0517 (3)	0.0552 (4)	−0.0002 (1)	F_7	0.0504 (2)	0.038 (2)	0.0399 (3)	0.0026 (1)	F_7	0.1388 (1)	0.1089 (2)	0.1192 (4)	0.0128 (3)
F_8	0.0744 (7)	0.0572 (7)	0.0589 (7)	−0.0248 (7)	F_8	0.0554 (5)	0.0414 (5)	0.0424 (5)	−0.022 (7)	F_8	0.1422 (3)	0.1087 (1)	0.1147 (1)	−0.0118 (2)
F_9	0.0659 (1)	0.0515 (2)	0.0551 (3)	0.003 (2)	F_9	0.0584 (7)	0.0451 (7)	0.0473 (7)	−0.0098 (3)	F_9	0.1451 (7)	0.1168 (8)	0.1307 (9)	0.0302 (8)
F_{10}	0.0679 (4)	0.0522 (4)	0.055 (2)	−0.0076 (3)	F_{10}	0.0581 (6)	0.0441 (6)	0.0459 (6)	−0.0162 (6)	F_{10}	0.1437 (5)	0.1135 (6)	0.1247 (8)	0.0157 (6)

(x) indicated the position when the error is considered and compared between functions.

When *BPH* are analyzed, the best fitting function was F_6. When considering *BPF*, F_2 was the expression with less error but the F_6 is near such as *BEH* case. However, considering the analysis developed by [10], F_6 was chosen to define the characteristic curve of the machine when other methods were compared to define the *BEH*, *BPH* and *BPF*. This comparison will show in Section 3.2. Therefore, when the head curve is defined the function will be the following expression:

$$H = \left[-0.69\left(\alpha\frac{Q}{Q_{BEP}}\right) + 0.122\left(\frac{Q}{Q_{BEP}}\right)^2 + 0.313\left(\frac{Q}{Q_{BEP}}\right) + 1.222\alpha^2 - 1.267\alpha + 1.294\right](Am^2 + Bm + C)Q^2 \quad (28)$$

Besides, F_6 includes both ratio of the rotational speed (α) and the ratio between Q/Q_{BEP}. The 'α' parameter also did other formulations in the published literature. Besides, this study adds another parameter, Q/Q_{BEP}. It considers the distance to the working zone of the maximum efficiencies).

Table 7 shows the average errors for *RMSE*, *MAD*, *MRD* and *BIAS* when the non−dimensional value of he/q^2 is calculated. In this case, F_6 was the expression, in which the errors were low when *BEH* and *BPH* are observed. In all cases, *BIAS* values were

low, and this index was between 0 and ±3%. These values are no significant because they show average errors, which are less than 3% when the head curve and power curve are estimated.

To develop the comparison of methods, F_6 was chosen to define the power curve of the machine, according to the expression shown in Table 1. The following expression enables estimating the power when the head curve and efficiency curve are known in nominal conditions.

$$P = \left[0.993\left(\alpha\frac{Q}{Q_{BEP}}\right) - 0.494\left(\frac{Q}{Q_{BEP}}\right)^2 - 0.156\left(\frac{Q}{Q_{BEP}}\right) - 0.471\alpha^2 + 0.38\alpha + 0.73\right] 9.81 \cdot \eta_0 (Am^2 + Bm + C)Q^3 \quad (29)$$

3.2. Comparison of the Proposal Study vs. Other Published Methods Applied to BEH, BPH and BPF

The proposed methodology was compared with five different published methods. These were: (i) classical affinity laws [18]; (ii) Carravetta et al. [22]; (iii) Fecarotta et al. [20]; (iv) Pérez−Sánchez et al. [17]; and (v) Tahani et al. [11].

$$Affinity\ Laws \begin{cases} h = ^2 \\ q = \alpha \\ p = \alpha^3 \\ e = 1 \end{cases}$$

$$Carraveta\ et\ al.,\ (2014) \begin{cases} h = 1.0253\alpha^{1.5615} \\ q = 1.0323\alpha^{0.7977} \\ p = 0.9741\alpha^{2.3207} \\ e = -0.4013\alpha^2 + 0.845\alpha + 0.5606 \end{cases}$$

$$Fecarotta\ et\ al.,\ (2016) \begin{cases} h = 0.972\alpha^{1.603} \\ q = 1.004\alpha^{0.825} \\ p = -- \\ e = -0.317\alpha^2 + 0.587\alpha + 0.707 \end{cases}$$

$$Perez - Sanchez\ et\ al.,\ (2018) \begin{cases} h = 1.89\alpha^2 - 1.54\alpha + 0.74 \\ q = 1.08\alpha^{0.7} \\ p = 4.59\alpha^2 - 6.33\alpha + 2.50 \\ e = -0.36\alpha^2 - 0.69\alpha + 0.66 \end{cases}$$

$$Tahani\ et\ al.,\ (2020) \begin{cases} h = 0.9962\alpha^{1.0851} \\ q = 0.9974\alpha^{0.3651} \\ p = 0.9767\alpha^{1.4888} \\ e = -4.3506\alpha^2 + 8.8879\alpha - 3.544 \end{cases}$$

The last cited methods were operated to get the best efficiency head, best power head and best power flow. The *BEH*, BPH and *BPF* for each method were compared with the experimental database for each machine. In all cases, when the average error indexes were calculated, the proposal of non−dimensional parameters (i.e., h/q^2 and he/q^2) showed the minor error values of *BEH*, *BPH* and *BPF*.

Figure 4a,b shows error indexes classified in the different methods. When the non−dimensional parameter, (he/q^2), is observed similar results were obtained. The proposed functions were the best compared to the other five methods. *RMSE*, *MAD* and *MRD* were 0.067, 0.051 and 0.054, respectively. When these error indexes were compared with the second-best value (affinity laws or Carravetta's method), the error values decreased between 26.5, 28.8 and 25.4%. For *BPH*, the trend of the results was similar. The proposed method was the most accurate, decreasing the errors between 25 and 32% compared with the second-best-option functions (Carravetta's). When *BPF* was analyzed, *RMSE*, *MAD* and *MRD* decreased 14.3, 12.4 and 13.4%, respectively. The use of MOALs demonstrated better accuracy in the operational curves when these results are compared with the affinity laws,

which are simpler, but they showed higher errors [11,17,19,22]. Figure 4 shows the decrease of the error in the different curves. Therefore, although the expressions use high degree equations, they improve the simulation of the PATs when they operate under variable rotational speeds.

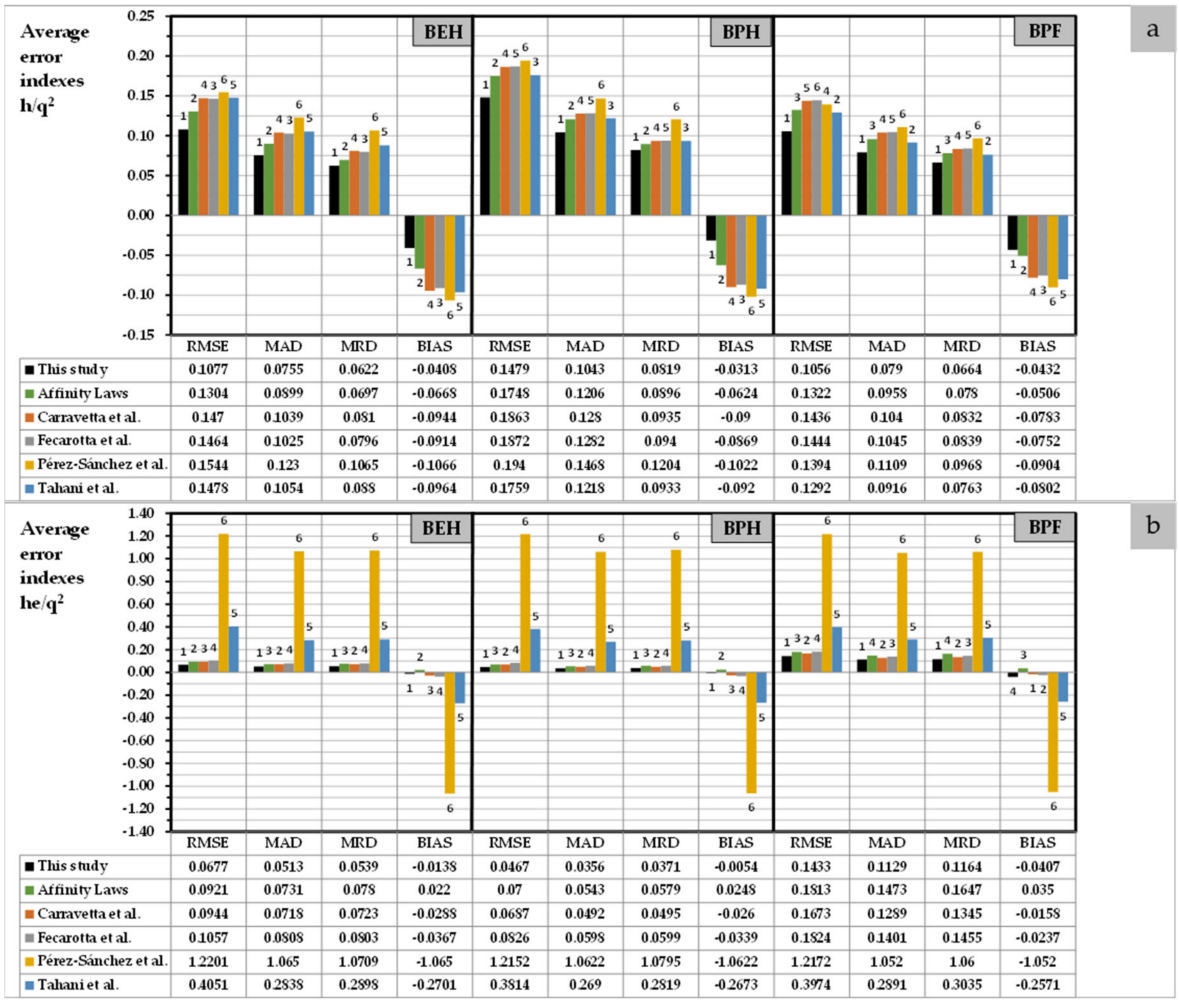

a	RMSE	MAD	MRD	BIAS	RMSE	MAD	MRD	BIAS	RMSE	MAD	MRD	BIAS
This study	0.1077	0.0755	0.0622	-0.0408	0.1479	0.1043	0.0819	-0.0313	0.1056	0.079	0.0664	-0.0432
Affinity Laws	0.1304	0.0899	0.0697	-0.0668	0.1748	0.1206	0.0896	-0.0624	0.1322	0.0958	0.078	-0.0506
Carravetta et al.	0.147	0.1039	0.081	-0.0944	0.1863	0.128	0.0935	-0.09	0.1436	0.104	0.0832	-0.0783
Fecarotta et al.	0.1464	0.1025	0.0796	-0.0914	0.1872	0.1282	0.094	-0.0869	0.1444	0.1045	0.0839	-0.0752
Pérez-Sánchez et al.	0.1544	0.123	0.1065	-0.1066	0.194	0.1468	0.1204	-0.1022	0.1394	0.1109	0.0968	-0.0904
Tahani et al.	0.1478	0.1054	0.088	-0.0964	0.1759	0.1218	0.0933	-0.092	0.1292	0.0916	0.0763	-0.0802

b	RMSE	MAD	MRD	BIAS	RMSE	MAD	MRD	BIAS	RMSE	MAD	MRD	BIAS
This study	0.0677	0.0513	0.0539	-0.0138	0.0467	0.0356	0.0371	-0.0054	0.1433	0.1129	0.1164	-0.0407
Affinity Laws	0.0921	0.0731	0.078	0.022	0.07	0.0543	0.0579	0.0248	0.1813	0.1473	0.1647	0.035
Carravetta et al.	0.0944	0.0718	0.0723	-0.0288	0.0687	0.0492	0.0495	-0.026	0.1673	0.1289	0.1345	-0.0158
Fecarotta et al.	0.1057	0.0808	0.0803	-0.0367	0.0826	0.0598	0.0599	-0.0339	0.1824	0.1401	0.1455	-0.0237
Pérez-Sánchez et al.	1.2201	1.065	1.0709	-1.065	1.2152	1.0622	1.0795	-1.0622	1.2172	1.052	1.06	-1.052
Tahani et al.	0.4051	0.2838	0.2898	-0.2701	0.3814	0.269	0.2819	-0.2673	0.3974	0.2891	0.3035	-0.2571

Figure 4. (**a**) Error indexes for the different methods applied to h/q^2; (**b**) error indexes for the different methods applied to he/q^2.

If h/q^2 (Figure 4a) is considered for *BEH*, the *RMSE*, *MAD* and *MRS* errors were 0.1077, 0.0755 and 0.622, respectively. These errors decreased between 17.4, 16 and 0.7% respectively, compared to the second-best method (affinity laws). If the *BPH* is analyzed similar results were obtained. The proposed functions were the best and the error indexes were reduced between 9 and 16% compared to the second−best method. When the error indexes were calculated for the *BPF*, the proposed study was the best, and the error values decreased 20.1, 17.5 and 14.9% for *RMSE*, *MAD* and *MRD* respectively.

When h/q^2 is analysed in Figure 4a, the proposed regression expression showed errors between 8.6% and 49.8% less than the obtained errors by application of the affinity laws, which was the second−best method for *BEH* and *BPH*, being the third when *BPF* was calculated. *RMSE* value was 0.1 for *BEH* and *BPF*, while it was 0.148 when *BPH* was estimated. If the *MAD* and *MRD* were analysed in this table, these values were around 0.07 and 0.06 respectively when *BEH* was compared. If *BPH* is compared, the *MAD* and *MRD* errors 0.1 and 0.08 respectively when they were 0.12 and 0.09 when the second−best method (affinity laws) is compared.

A similar analysis can be developed by looking at Figure 4b. The proposed expression regressions were the best when *BEH*, *BPH* and *BPF* were defined using all previous cited methods and the errors calculated. If *BEH* is analyzed, the proposed expressions in this research reduced the error indexes (*RMSE*, *MAD* and *MRD*) by around 30% compared to Affinity laws and Carravetta's method, which were the second and third best methods for this *BEH* curve. In this curve, the *BIAS* was near −1%. If *BPH* is analyzed, a similar analysis was done. The error indexes reduced between 33 and 36% the error of the second−best method, while the *BIAS* value was 0.5% for *BPH*. Finally, if *BPF* is observed, the proposed expressions decreased the error indexes. Particularly, *RMSE*, *MAD* and *MRD* decreased 21, 23 and 30% respectively between the proposed method and Carravetta's method.

If *BPF* is analyzed, *RMSE* error was 0.14. It decreased by 14% compared to the second−best method (Carravetta´s method). *MAD* and *MRD* got similar values, which were reduced by 12.4 and 14.1%, respectively.

Both parameters, h/q^2 and he/q^2 showed the proposed regression using F_6 enabled to estimate the best efficiency head, best power head and best power flow. Three lines are strategic considerations when water managers define operations rules to maximize the energy recovery using micro hydropower systems.

3.3. Application of the Proposed Curves to Experimental Machine

The proposed empirical regressions were applied to a tested experimental machine to show the accuracy of the expressions applied in real case studies. In this case, the tested machine was NK−140 125/127 [28], being a specific speed in turbine mode of 31.16 rpm (m, kW). Its *BEP* operating as the turbine was 17.99 l/s, 30.31 m w.c. with an efficiency of 0.695. The machine was tested on six different rotational speed, being 3000 rpm its nominal rotational speed. Figure 5a shows the head as a function of the flow of the *BEH*. The m value for this machine is 0.056. If this curve is analyzed, Figure 5b shows the curve, which defines the power as a function of the flow. Both figures show good accuracy when making visual comparison. When the error was measured, *RMSE* and *MRD* were 0.077 and 0.059 respectively, being *BIAS* equal to 0.0585. If the head curve is analyzed using the proposed expressions in NK−140 125/127, the average error values of *RMSE* and *MRD* were 0.2195 and 0.0096, respectively. The error values decreased around 65.6% in both errors when they were compared to affinity laws. When the power curve is analyzed, *RMSE* and *MRD* were 0.0123 and 0.005 respectively. These errors decreased and *MRD* errors decreased around 82.6% compared to affinity laws. The expressions indicate the good fit for the whole range of n_{st} when Figures 4 and 5 are considered and the errors are evaluated.

Figure 5c shows the operation curve (H−Q), representing the best power head. This is the most important curve since the operation based on this curve is the best to maximize the recovered energy, when variable operation strategy is applied in a water pressurized systems. Comparison of the power curve between the estimated and experimental *BPH* values (Figure 5d) also shows a good fit.

Figure 5e,f show the difference between trend parabolas and tested curves when *BEH*, *BPH* and *BPF* were considered both the curves (i.e., head and power curve). These three curves (i.e., *BEH*, *BPH* and *BPF*) are the curves, which should be considered when regulation strategies want to be considered to maximize the recovered energy.

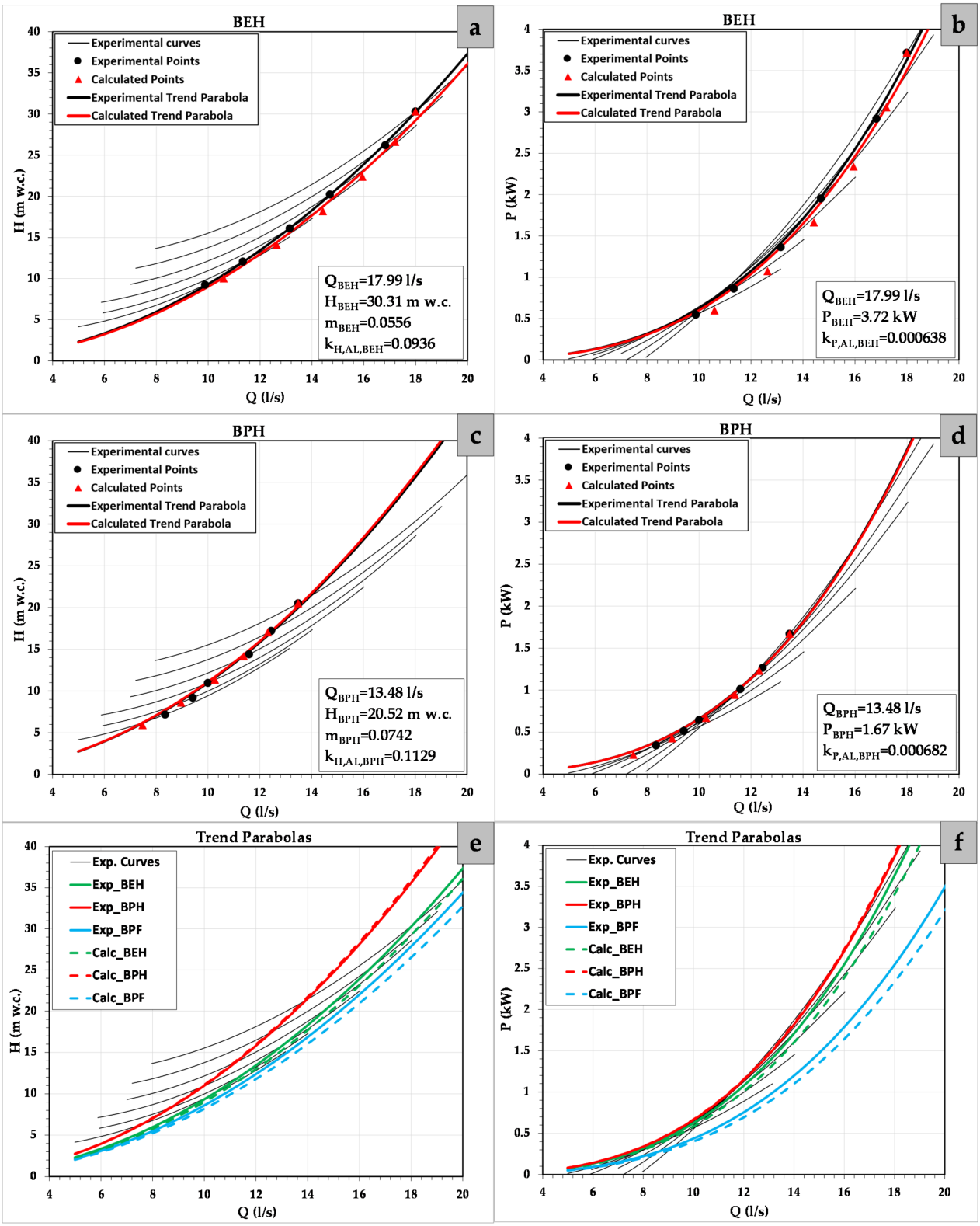

Figure 5. (**a**) H−Q for *BEH*; (**b**) P−Q for *BEH*; (**c**) H−Q for *BPH*; (**d**) P−Q for *BPH*; (**e**) H−Q for *BEH*, *BPH* and *BPF*; (**f**) P−Q for *BEH*, *BPH* and *BPF*.

4. Conclusions

The present research proposed a new modification of the affinity laws (MOAL) when applied to pumps working as turbines. These new expressions were compared to the rest of the published methods and affinity laws, showing the best results in the estimation of the best efficiency head, best power head and best power flow. Analyses of these curves in other published researches showed that they are key in the operation of the recovery systems to maximize recovered energy. Therefore, the modified affinity laws proposed in this study were found to decrease the error indexes by 8 to 30% compared with existing methods, and can help water system managers to improve the accuracy of energy predictions.

The analysis of the different tested curves as well as the consideration of the analytical expressions showed the importance of the Q_{BPH} value. This value should be considered when the machine is chosen, and it is always greater than $Q_{0,\,min}$. Therefore, the PATs system could operate under the best power head conditions when the constrain '$Q_{0,\,min} \leq Q_{BPH}$' is satisfied.

Incorporating these curves (i.e., *BEH*, *BPH* and *BPF*) when the potential recovery is analyzed by water managers is crucial to get the best results, when the *BPH* achieves the best results in terms of recovered energy. However, the analysis of *BEH* and/or *BPF* is recommended because it can be useful when the recovered energy is not the main goal to be achieved and other factors such as valves regulation or sustainable measures are considered.

These MOAL were validated when the specific speeds of the PATs systems were between 5 and 50 rpm using 15 different machines and 87 different rotational speed. The analysis showed the need to increase the tests applied on axial machines to increase the operating range by the research community. Future researches should focus on developing axial machines analyses. These machines are significant in the water pressurized systems because there are many potential recovery points in which the flow is high, but the recoverable head is low, and therefore, the recovery systems should be established by axial machines.

Author Contributions: Conceptualization, P.A.L.-J. and M.P.-S.; methodology, C.A.M.Á. and F.-J.S.-R.; software, writing—original draft preparation, C.A.M.Á. and M.P.-S.; writing—review and editing, M.P.-S. and P.A.L.-J.; visualization M.P.-S.; supervision, P.A.L.-J. All authors have read and agreed to the published version of the manuscript.

Funding: This research received no external funding.

Institutional Review Board Statement: Not applicable.

Informed Consent Statement: Not applicable.

Data Availability Statement: Not applicable.

Conflicts of Interest: The authors declare no conflict of interest.

References

1. Da Silveira, A.P.P.; Mata-Lima, H. Energy audit in water supply systems: A proposal of integrated approach towards energy efficiency. *Water Policy* **2020**, *22*, 1126–1141. [CrossRef]
2. Postacchini, M.; Darvini, G.; Finizio, F.; Pelagalli, L.; Soldini, L.; Di Giuseppe, E. Hydropower generation through pump as turbine: Experimental study and potential application to small-scale WDN. *Water* **2020**, *12*, 958. [CrossRef]
3. Pugliese, F.; De Paola, F.; Fontana, N.; Giugni, M.; Marini, G. Experimental characterization of two Pumps As Turbines for hydropower generation. *Renew. Energy* **2016**, *99*, 180–187. [CrossRef]
4. Kim, J.W.; Suh, J.W.; Choi, Y.S.; Lee, K.Y.; Kim, J.H.; Kanemoto, T.; Kim, J.H. Simultaneous efficiency improvement of pump and turbine modes for a counter-rotating type pump-turbine. *Adv. Mech. Eng.* **2016**, *8*, 1–14. [CrossRef]
5. Binama, M.; Su, W.T.; Li, X.B.; Li, F.C.; Wei, X.Z.; An, S. Investigation on pump as turbine (PAT) technical aspects for micro hydropower schemes: A state-of-the-art review. *Renew. Sustain. Energy Rev.* **2017**, *79*, 148–179. [CrossRef]
6. Ortiz Flórez, R.; Abella Jiménez, J. Máquinas Hidráulicas Reversibles Aplicadas a Micro Centrales Hidroeléctricas. *IEEE Lat. Am. Trans.* **2008**, *6*, 170–175.
7. Sharma, K. *Small Hydroelectric Project-Use of Centrifugal Pumps as Turbines*; Kirloskar: Bangalore, India, 1985.

8. Derakhshan, S.; Nourbakhsh, A. Experimental study of characteristic curves of centrifugal pumps working as turbines in different specific speeds. *Exp. Therm. Fluid Sci.* **2008**, *32*, 800–807. [CrossRef]
9. Pérez-Sánchez, M.; Sánchez-Romero, F.J.; Ramos, H.M.; López-Jiménez, P.A. Improved Planning of Energy Recovery in Water Systems Using a New Analytic Approach to PAT Performance Curves. *Water* **2020**, *12*, 468. [CrossRef]
10. Plua, F.A.; Sánchez-Romero, F.J.; Hidalgo, V.; López-Jiménez, P.A.; Pérez-Sánchez, M. New expressions to apply the variation operation strategy in engineering tools using pumps working as turbines. *Mathematics* **2021**, *9*, 860. [CrossRef]
11. Tahani, M.; Kandi, A.; Moghimi, M.; Houreh, S.D. Rotational speed variation assessment of centrifugal pump-as-turbine as an energy utilization device under water distribution network condition. *Energy* **2020**, *213*, 118502. [CrossRef]
12. Chen, S.; Chen, B. Urban energy–water nexus: A network perspective. *Appl. Energy* **2016**, *184*, 905–914. [CrossRef]
13. Carravetta, A.; Del Giudice, G.; Fecarotta, O.; Ramos, H. Pump as Turbine (PAT) Design in Water Distribution Network by System Effectiveness. *Water* **2013**, *5*, 1211–1225. [CrossRef]
14. Ebrahimi, S.; Riasi, A.; Kandi, A. Selection optimization of variable speed pump as turbine (PAT) for energy recovery and pressure management. *Energy Convers. Manag.* **2021**, *227*, 113586. [CrossRef]
15. Man, Y.; Han, Y.; Liu, Y.; Lin, R.; Ren, J. Multi-criteria decision making for sustainability assessment of boxboard production: A life cycle perspective considering water consumption, energy consumption, GHG emissions, and internal costs. *J. Environ. Manag.* **2020**, *255*, 109860. [CrossRef]
16. Niet, T.; Arianpoo, N.; Kuling, K.; Wright, A.S. Embedding the United Nations sustainable development goals into energy systems analysis: Expanding the food–energy–water nexus. *Energy Sustain. Soc.* **2021**, *11*, 1–12. [CrossRef]
17. Pérez-Sánchez, M.; López-Jiménez, P.A.; Ramos, H.M. Modified Affinity Laws in Hydraulic Machines towards the Best Efficiency Line. *Water Resour. Manag.* **2018**, *32*, 829–844. [CrossRef]
18. Mataix, C. *Turbomáquinas Hidráulicas*; Universidad Pontificia Comillas: Madrid, Spain, 2009; ISBN 978-84-8468-252-3.
19. Fecarotta, O.; Carravetta, A.; Ramos, H.M.; Martino, R. An improved affinity model to enhance variable operating strategy for pumps used as turbines. *J. Hydraul. Res.* **2016**, *54*, 332–341. [CrossRef]
20. Hyypiä, J. Hydraulic energy recovery by replacing a control valve with a centrifugal pump used as a turbine. Ph.D. Thesis, Lappeenranta University of Technology, Lappeenranta, Finland, 2016.
21. Nygren, L. Hydraulic Energy Harvesting with Variable-Speed-Driven Centrifugal Pump as Turbine. Master's Thesis, Lappeenranta University of Technology, Lappeenranta, Finland, 2017.
22. Carravetta, A.; Conte, M.C.; Fecarotta, O.; Ramos, H.M. Evaluation of PAT performances by modified affinity law. *Procedia Eng.* **2014**, *89*, 581–587. [CrossRef]
23. KSB. "PATs Curves," Catalogue. 2019. Available online: https://www.ksb.com/es-es/productos/catalogo-de-productos (accessed on 5 July 2021).
24. Jain, S.V.; Swarnkar, A.; Motwani, K.H.; Patel, R.N. Effects of impeller diameter and rotational speed on performance of pump running in turbine mode. *Energy Convers. Manag.* **2015**, *89*, 808–824. [CrossRef]
25. Abazariyan, S.; Rafee, R.; Derakhshan, S. Experimental study of viscosity effects on a pump as turbine performance. *Renew. Energy* **2018**, *127*, 539–547. [CrossRef]
26. Kramer, M.; Terheiden, K.; Wieprecht, S. Pumps as turbines for efficient energy recovery in water supply networks. *Renew. Energy* **2018**, *122*, 17–25. [CrossRef]
27. Delgado, J.; Ferreira, J.P.; Covas, D.I.C.; Avellan, F. Variable speed operation of centrifugal pumps running as turbines. Experimental investigation. *Renew. Energy* **2019**, *142*, 437–450. [CrossRef]
28. Stefanizzi, M.; Torresi, M.; Fortunato, B.; Camporeale, S.M. Experimental investigation and performance prediction modeling of a single stage centrifugal pump operating as turbine. *Energy Procedia* **2017**, *126*, 589–596. [CrossRef]